HHS Public Access

Author manuscript

Stem Cell Res. Author manuscript; available in PMC 2019 December 18.

Published in final edited form as:

Stem Cell Res. 2018 December ; 33: 199–205. doi:10.1016/j.scr.2018.10.020.

A20 deficiency in multipotent progenitors perturbs quiescence of hematopoietic stem cells

Masahiro Marshall Nakagawa[a], **Harry Davis**[b], **Chozha Vendan Rathinam**[a,b,c,d,*]

[a]Department of Genetics and Development, Columbia University Medical Center, 701 W 168th street, New York, NY 10032, United States

[b]Institute of Human Virology, 725 W Lombard Street, University of Maryland, School of Medicine, Baltimore, MD 21201, United States

[c]Center for Stem Cell & Regenerative Medicine, 725 W Lombard Street, University of Maryland, School of Medicine, Baltimore, MD 21201, United States

[d]Marlene & Stewart Greenebaum Comprehensive Cancer Center, 725 W Lombard Street, University of Maryland, School of Medicine, Baltimore, MD 21201, United States

Abstract

Inflammatory signals have been shown to play a critical role in controlling the maintenance and functions of hematopoietic stem cells (HSCs). While the significance of inflammation in hematopoiesis has begun to unfold, molecular mechanisms and players that govern this mode of HSC regulation remain largely unknown. The E3 ubiquitin ligase A20 has been considered as a central gatekeeper of inflammation. Here, we have specifically depleted A20 in multi-potent progenitors (MPPs) and studied its impact on hematopoiesis. Our data suggest that lack of A20 in $Flt3^{+}$ progenitors causes modest alterations in hematopoietic differentiation. Analysis of hematopoietic stem and progenitor cell (HSPC) pool revealed alterations in HSPC subsets including, HSCs, MPP1, MPP2, MPP3 and MPP4. Interestingly, A20 deficiency in MPPs caused loss of HSC quiescence and compromised long-term hematopoietic reconstitution. Mechanistic studies identified that A20 deficiency caused elevated levels of Interferon-γ signaling and downregulation of p57 in HSCs. In essence, these studies identified A20 as a key regulator of HSC quiescence and cell fate decisions.

1. Introduction

Hematopoietic Stem Cells (HSCs) are believed to be largely quiescent under steady state conditions and enter into an actively proliferating state in response to external cues. In

*Corresponding author at: Laboratory for Stem Cell & Cancer Biology, Center for Stem Cell Biology & Regenerative Medicine, Marlene & Stewart Greenebaum Comprehensive Cancer Center, Institute of Human Virology, University of Maryland School of Medicine, 725 West Lombard Street, Room # S315 (Office), Room # S314 & # S333 (Lab), Baltimore, MD 21201, United States. crathinam@ihv.umaryland.edu (C.V. Rathinam).

Author contributions

Contribution: M.M.N performed research, collected data and interpreted data; H.D. provided help with animal experiments; C.V.R. designed and performed research, interpreted data and wrote the manuscript.

Supplementary data to this article can be found online at https://doi.org/10.1016/j.scr.2018.10.020.

the recent years, role of infection and inflammation in the control of hematopoiesis have gained a lot of attention. HSCs have been evolved to sense infections either through direct contact with the pathogens via the Toll Like receptor (TLR) pathways or through actions of inflammatory cytokines produced by the effector cells of the immune system and hematopoietic progenitors (Baldridge et al., 2010; Baldridge et al., 2011; Weiner et al., 2008). A spectrum of pro-inflammatory cytokines and chemokines, that includes IL1, IL6, IL8, TNF, CC-Chemokine ligand 2 (CCL2), IFN-α and IFN-γ, has been identified to regulate HSCs and hematopoiesis. In particular, chronic exposure of HSCs to interferons (both α and γ) results in compromised self-renewal and quiescence of HSCs.

A20 (also known as Tnfaip3) acts as an ubiquitin editing enzyme and has emerged as a key anti-inflammatory molecule of the immune system. A20 contains an amino (N)-terminal cysteine protease/DUB domain (that is necessary for the deubiquitylating functions) and a carboxyl (C)-terminal zinc finger (ZNF) domain (which confers the E3 ubiquitin ligase functions) (Wertz et al., 2004). A20 catalyzes the K48-linked ubiquitylation of target proteins through its caboxy-terminal ZNF domain, therefore it directs its targets for proteasomal degradation. In addition, A20 removes K63–linked ubiquitin chains from its target proteins, which not only inactivates the signaling function of the targets but might also facilitate its K48- linked ubiquitylation and degradation (Wertz et al., 2004). The negative signaling function of A20 involves deconjugation of K63–linked ubiquitin chains from TRAF6 and RIP1, which are central players of the toll like receptor (TLR) and Tumor necrosis factor receptor (TNFR) pathways (Sun, 2008). In addition, A20 also mediates deubiquitylation of RIP2 and thereby negatively regulating the activation of NF-kB and the induction of pro-inflammatory cytokines (Hitotsumatsu et al., 2008; Hymowitz and Wertz, 2010; Sun, 2008; Vereecke et al., 2009). Functions of A20 in many cell types of the immune system have been clearly established, however, its role in hematopoiesis remains largely unknown. We have recently identified that A20 deficiency in HSCs leads to loss of its pool, pathologic hematopoiesis, including auto-inflammatory disease, myeloproliferation and lymphopenia, and postnatal lethality that are dependent on IFNγ (Nakagawa et al., 2015). In the present study, we specifically ablated A20 in ($Flt3^{+}$) multi-potent progenitors (MPPs), but not in HSCs, and our data identified that presence of A20 in HSCs is sufficient and necessary to prevent autoinflammatory disorders. In addition, the current study demonstrates that lack of A20 is sufficient to affect HSC pool and quiescence.

2. Results

To study the role of A20 in hematopoietic differentiation, we crossed A20 floxed mice (Nakagawa et al., 2015) with $Flt3^{cre/+}$ (Benz et al., 2008) transgenic mice to generate $A20^{F/F}Flt3^{cre/+}$ mice (henceforth referred to as KO) Flt3 Cre has been shown to induce recombination in all hematopoietic lineage, including myeloid erythroid and lymphoid, cells starting from MPPs ($Flt3^{+}$ LSK) (Boyer et al., 2011). Analysis of hematopoietic organs from KO mice indicated elevated, but statistically insignificant, cellularity of BM and spleen, and relatively normal cell counts in thymus (Fig. 1A). Determination of recombination efficiencies by PCR indicated A20 deletion in majority of BM cells of KO mice (Fig. 1B). Consistently, flow cytometric analysis of $A20^{F/F}Rosa^{RFP}Flt3^{cre/+}$ mice revealed deletion efficiencies (as inferred by RFP expression) of > 75% in BM, spleen, thymus and peripheral

blood of KO mice (Fig. 1C). Our analysis of RFP expression in various hematopoietic progenitor subsets in the BM identified that majority (> 90%) of $CD150^+CD48^-LSK$ cells (a subset that is enriched for HSCs and MPP1 (Cabezas-Wallscheid et al., 2014; Wilson et al., 2008)), were RFP^- and that all the other downstream hematopoietic subsets, including $CD150^+CD48^+$ LSK (a subset enriched for MPP2) and $CD150^+CD48^+$ LSK (a subset enriched for MPP3 & MPP4), show remarkable expression of RFP (Fig. 1D, E). These data are consistent with earlier studies that Flt3 Cre mouse strain does not induce recombination in LT-HSCs (Boyer et al., 2011). First, we assessed multi-lineage hematopoietic differentiation in KO by flow cytometry and the data indicated increased proportions of $CD11b^+$ myeloid lineage cells and $CD3e^+$ T lineage cells, reduced proportion of $CD19^+$ B lineage cells, and normal frequencies of $Ter119^+$ erythroid lineage cells in the BM of KO mice (Fig. 1F). However, determination of absolute cell counts revealed normal numbers of myeloid/erythroid lineage cells, reduction of B cells, and modestly increased numbers of T cells in the BM of KO mice (Fig. 1G). On the other hand, both relative and absolute frequencies of myeloid, erythroid and T cells were normal in the spleen of KO mice (Fig. 1H, I). Whereas the frequencies of B cells in the KO spleen were modestly decreased, their absolute numbers were normal (Fig. 1H, I). Analysis of thymus of KO mice revealed intact thymic differentiation with normal frequencies and numbers of $CD4^-CD8^-$; $CD4^+CD8^+$; $CD4^+CD8^-$; and $CD4^-CD8^+$ cells (Fig. 1J). Finally, analysis of peripheral blood indicated normal frequencies of myeloid ($CD11b^+$) cells and T ($CD3e^+$) cells, but reduced frequencies of B ($CD19^+$) cells (Fig. 1K). Taken together, these data indicated that deletion of A20 at the MPP stage causes only modest alterations in hematopoietic differentiation.

Next, we studied the hematopoietic stem and progenitor cell (HSPC) compartments in the BM of KO mice. Analysis of $Lin^-Sca1^+c\text{-}Kit^+$ (LSK) cells of the BM from KO mice indicated; a significant increase in absolute numbers, but normal relative numbers, of $CD34^-Flt3^-LSK$ subset; an increase in both relative and absolute numbers of $CD34^+Flt3^-LSK$ subset; and a decrease in relative numbers, but an increase in absolute numbers, of $CD34^+Flt3^+LSK$ subset (Fig. 2A, C, D). To further characterize the LSK subset, based on CD150 and CD48 expression, we followed a more refined immunophenotyping scheme of HSCs and MPPs (Cabezas-Wallscheid et al., 2014; Wilson et al., 2008). Our analysis identified; a decrease in relative numbers and an increase in absolute numbers of $CD150^+CD48^-LSK$ subset (a fraction that is enriched for LT-HSCs and MPP1); an increase in both relative and absolute numbers of $CD150^+CD48^+$ LSK subset (a fraction that is enriched for MPP2); and a decrease in relative numbers, but an increase in absolute numbers, of $CD150^-CD48^+$ LSK subset (a fraction that is enriched for MPP3 & MPP4) (Fig. 2A, E, F). Further enrichment of these subsets into HSCs ($CD150^+CD48^-CD34^-Flt3^-LSK$), MPP1($CD150^+CD48^-CD34^+Flt3^-LSK$), MPP2 ($CD150^+CD48^+CD34^+Flt3^-LSK$), MPP3 ($CD150^-CD48^+CD34^+Flt3^-LSK$) and MPP4 ($CD150^-CD48^+CD34^+$ $Flt3^+LSK$) subsets revealed; a relative decrease, but normal absolute numbers of HSCs; normal relative and absolute numbers of MPP1; normal relative numbers, but increased absolute numbers of MPP2; increased relative and absolute numbers of MPP3; and decreased relative number, but normal absolute numbers of MPP4 (Fig. 2G–I). Overall,

these studies specified that A20 deletion in $Flt3^{+}$ progenitors disturbs the maintenance of HSPC pool.

To test if this altered distribution of the HSPC pool results in compromised HSC functions, we first performed a series of bone marrow transplantation (BMT) studies. Transfer of RBC depleted total BM from either control or A20 KO into lethally irradiated congenic (CD45.1) recipients resulted in normal radioprotection (Suppl. Fig. 1A, B) and development of donor derived hematopoiesis at 8 weeks of transplantation (Suppl. Fig. 1C). BMT studies using BM of $A20^{+/+}$ $ROSA^{RFP}$ $Flt3^{Cre/+}$ or $A20^{F/F}$ $ROSA^{RFP}$ $Flt3^{Cre/+}$ mice as donors indicated that majority of the A20 KO derived cells (RFP^{+}) underwent recombination (Suppl. Fig. 1D). Multi-lineage analysis indicated comparable frequencies of myeloid cells, B cells and T cells within RFP^{+} cells (Suppl. Fig. 1E).

Consistently, competitive repopulation studies (Suppl. Fig. 1F) indicated comparable levels of donor derived hematopoiesis (Suppl. Fig. 1G). Multi-lineage hematopoiesis in the peripheral blood of recipients that received BM of either control ($CD45.2^{+}$; $A20^{+/+}$ $ROSA^{RFP}$ $Flt3^{Cre/+}$) + competitive (CD45.1) mice or KO ($CD45.2^{+}$; $A20^{F/F}$ $ROSA^{RFP}$ $Flt3^{Cre/+}$ mice) + competitive (CD45.1) mice indicated comparable frequencies of myeloid cells, B cells and T cells (Suppl. Fig. 1H).

To assess the long-term reconstitution abilities of KO HSCs, we performed secondary transplantations (Fig. 3A). Transfer of BM of primary recipients (WT; $CD45.1^{+}$), that received either control or A20 KO BM 12 weeks before, into lethally irradiated secondary recipients (WT; $CD45.1^{+}$) caused a modest, but not statistically significant, loss of radioprotection (Fig. 3B). Analysis of donor derived chimera in the peripheral blood of secondary recipients after 12 weeks of transplantation revealed a modest decrease of KO (CD45.2) derived hematopoiesis (Fig. 3C). Multi-lineage analysis indicated that donor (CD45.1) derived myeloid cells were normal (Fig. 3D). However, donor derived B cells ($CD19^{+}$) and T cells ($CD3\varepsilon^{+}$) were reduced in the peripheral blood of secondary recipients that received KO BM (Fig. 3D). Overall these data indicate that A20 deficiency in MPPs affects the long-term, but not reconstitutional abilities of HSCs.

To identify physiological alterations that might contribute to the altered distribution of HSPC pool in A20 KO mice, we performed apoptosis and quiescence studies. Maintenance of the HSPC pool has been shown to be tightly regulated through apoptosis and quiescence (Cheung and Rando, 2013). Flow cytometric analysis indicated normal frequencies of apoptosis between control and A20 deficient HSPCs (Fig. 3E). Next, we performed quiescence studies using 3 independent approaches. First, we measured cell cycle through Hoechst and Pyronin Y staining (Shen et al., 2008) and data indicated that the frequencies of quiescent ($Hoechst^{low}$ $Pyronin\ Y^{low}$) cells were reduced in the HSPC compartment of A20 KO mice (Fig. 3F). Second, we measured cell cycle status using Ki67 and Hoechst (Kim and Sederstrom, 2015) and data revealed that the frequencies of cells in G0 (Quiescent) phase were reduced and in G2/S phase were increased in HSPC compartment of A20 deficient mice (Fig. 3G, H). Similarly, the frequencies of G0 cells were reduced, albeit not significant, and of cells in G2/S phase were remarkably increased in the $CD150^{+}CD48^{-}$ LSK (HSC and MPP1 enriched subset) cells of A20 deficient mice (Fig. 3I, J). Third, we

performed BrdU incorporation studies to directly measure proliferation of HSPC subsets. Consistent with our Ki67 and Hoechst studies, the frequencies of proliferating cells were more in LSK, $CD150^{+}CD48^{-}$LSK, $CD34^{+}Flt3^{-}$LSK and $CD34^{+}Flt3^{+}$LSK subsets (Fig. 3K, L). These studies have unequivocally demonstrated that A20 deficiency in MPPs causes loss of quiescence in all subsets of HSPCs.

To identify mechanisms through which A20 deficiency affects HSC quiescence, we performed gene expression studies. Based on the previous findings (Baldridge et al., 2010; Baldridge et al., 2011; Essers et al., 2009; King and Goodell, 2011; Mirantes et al., 2014; Sato et al., 2009), including our own (Nakagawa et al., 2015), on the critical role of inflammatory cytokines in HSC quiescence, we have hypothesized that exaggerated expression levels of inflammatory cytokines might be responsible for the loss of HSC quiescence in A20 deficient HSCs. Real-Time PCR analyses on total bone marrow cells suggested normal expression levels of many NF-κB targets, except a modest upregulation of NF-κBIα and a downregulation of BclXL, in the BM of A20 deficient mice (Fig. 4A). While expression levels of IL-6 and TNF-α were normal, a remarkable upregulation of interferon (IFN)γ and a modest down-regulation of IFN-α were noticed in the total BM of A20 deficient mice (Fig. 4A). Consistent with increased IFNγ mRNA expression in the BM, IFNγ levels in the blood serum were elevated in KO mice (Fig. 4B).

Previous studies established that increased IFN-γ signals cause increased surface expression of Seal in HSPCs (King and Goodell, 2011; Snapper et al., 1991). Our analysis of A20 deficient HSPCs revealed a marked upregulation of Sca1 in the surface of Lin^{-}c-$Kit^{+}CD150^{+}$ cells (Fig. 4C). In agreement with elevated IFN-γ, expression levels of its down targets including Irf1, Irgm1 and Stat1 were elevated in $Flt3^{+}$LSK cells and $CD150^{+}CD48^{-}$LSK cells of KO mice (Fig. 4D, E), even though expression levels of many NF-κB targets were normal in $Flt3^{+}$ LSK cells (Fig. 4 D). Amongst other molecular targets of IFN-γ (de Bruin et al., 2013), we focused on the expression levels of p57. Interestingly, expression levels of p57 were reduced in A20 deficient $Flt3^{+}$ LSK cells and $CD150^{+}CD48^{-}$LSK cells (Fig. 4 D, E). In keeping with our findings loss of p57 in HSCs results in reduced quiescence and functions of HSCs (Matsumoto et al., 2011). In essence these studies suggest that A20 deficiency in MPP causes elevated IFN-γ expression, and therefore its signaling cascade in HSCs, which eventually may result in the loss of HSC quiescence.

3. Discussion

In the present study we show that deletion of A20 in $Flt3^{+}$ hematopoietic progenitor cells ($A20^{Flt3\text{-}KO}$) resulted in altered distribution of HSPC subsets, including HSCs. While loss of HSC quiescence was noticed in $A20^{Flt3\text{-}KO}$ mice, this did not impair the short-term repopulation capacities of HSCs and caused only modest reduction in long-term hematopoietic reconstitution functions of HSCs. Interestingly, A20 deficiency in MPPs did not result in overt hematopoietic abnormalities or pathological hematopoiesis. In particular, we did not observe systemic inflammation, lymphopenia and myeloproliferation, even though modest changes in B cell numbers were noticed in hematopoietic organs. These findings were unexpected based on our previous studies on A20 deficient mice

(Nakagawa et al., 2015). We previously reported that A20 deficiency in HSCs ($A20^{Hem\text{-}KO}$) resulted in a severe and lethal phenotype; including premature death, systemic inflammation, hepatomegaly, splenomegaly, reduced HSC quiescence and loss of HSC pool and functions (Nakagawa et al., 2015). On the other hand, analysis of HSC compartment of $A20^{Flt3\text{-}KO}$ mice indicated increased absolute numbers of HSPC subsets, including $CD150^{+}CD48^{-}LSK$, $CD34^{+}Flt3^{-}LSK$ and $CD34^{+}Flt3^{+}LSK$ fractions. This observation was conflicting with our previous findings that $CD150^{+}CD48^{-}LSK$ pool and $CD34^{+}Flt3^{+}LSK$ numbers were severely reduced in $A20^{Hem\text{-}KO}$ (Nakagawa et al., 2015). One possible explanation for these discrepancies could be that A20 functions are intact in HSCs of $A20^{Flt3\text{-}KO}$ mice, as A20 is deleted in hematopoietic cells after the $Flt3^{+}$ stage (i.e. in MPPs), whereas A20 gene is deleted in all hematopoietic cells, including LT-HSCs, of $A20^{Hem\text{-}KO}$ mice. Together these observations suggest that A20 functions in HSCs are critical for the suppression of lethal inflammatory disorders and that A20 is an essential for the maintenance and functions of HSPC pool.

Inflammatory cytokines, including IL1, IL6, TNFα, IFNα, and IFNγ, are shown to regulate hematopoiesis and the physiology of HSCs (Baldridge et al., 2010; Baldridge et al., 2011; Essers et al., 2009; King and Goodell, 2011; Mirantes et al., 2014; Sato et al., 2009). In particular, IFNγ plays a pivotal role in the maintenance of HSC pool and quiescence (Baldridge et al., 2010). Moreover, deregulated IFNγ signaling has been implicated in the pathogenesis of various hematopoietic abnormalities (de Bruin et al., 2014). Our previous studies on $A20^{Hem\text{-}KO}$ (Nakagawa et al., 2015) identified a key role for IFNγ in the onset of pathologic hematopoiesis (Nakagawa et al., 2015). Interestingly, complete ablation of IFNγ signals in $A20^{Hem\text{-}KO}$ mice resulted in a rescue of the inflammatory phenotype, including premature death, and the HSC phenotype (Nakagawa et al., 2015). Consistent with our data on $A20^{Hem\text{-}KO}$ (Nakagawa et al., 2015), in the current study, we noticed marked elevation of IFNγ, very likely due to increased NF-κB binding to IFNγ promoter (Nakagawa et al., 2015), in $A20^{Flt3\text{-}KO}$ mice. Increased signaling mediated by IFNγ has been shown to directly affect HSC quiescence by suppressing the expression levels of p57, a key regulator of HSC quiescence (Nakagawa et al., 2015). Our gene expression studies on the HSC subsets identified a striking down regulation of p57 in HSCs. These data suggest that deregulated IFNγ signals might be responsible for the loss of HSC quiescence in $A20^{Flt3\text{-}KO}$ mice, however, we cannot rule out the possible involvement of additional pathways.

The study presented here indicated that A20 deficiency in MPPs, is sufficient to alter LT-HSC pool and functions. Because A20 expression and functions are intact in LT-HSCs, we concluded that A20 deficiency affects HSCs in a cell extrinsic manner. Based on the compelling role of IFNγ in the cell extrinsic mode of HSC regulation, we speculate that the HSC phenotype of $A20^{Flt3\text{-}KO}$ mice is caused by IFNγ, as we demonstrated earlier (Nakagawa et al., 2015). Even though our studies have not specified the source of IFNγ in these settings, we assume that cells of the lymphoid lineage (as they are differentiated from the $Flt3^{+}$ hematopoietic progenitors), might be predominantly responsible for the elevated IFNγ in $A20^{Flt3\text{-}KO}$ mice. Future studies that aim to decipher the significance of IFNγ produced by the cells of the HSC microniche vs. systemic IFNγ produced by immune cells of lymphoid organs would be of great interest to understand the pathophysiological significance of IFNγ. In toto, the study presented here highlights the significance of

inflammatory pathways in regulating the HSC pool and identifies A20 as a key regulator of inflammation induced hematopoiesis.

4. Methods

4.1. Mice

Tnfaip3(A20)$^{flox/flox}$ mice were previously described (Nakagawa et al., 2015). Flt3$^{Cre/+}$ mice were generated and reported earlier (Benz et al., 2008). CD45.1 congenic animals were purchased from the National Cancer Institute. The Institutional Animal Care and Use Committee of Columbia University and University of Maryland School of Medicine approved all mouse experiments.

4.2. Flow cytometry

Cells were analyzed by flow cytometry with FACS Fortessa, LSR II (BD), Attune NXT and FACSDiva software (BD Biosciences) or FlowJo software (Tree Star). The following monoclonal antibodies were used: anti- CD34 (RAM34), anti-CD45.1 (A20), anti-CD45.2 (104), anti-CD48 (HM48-1), anti-CD117 (2B8), anti-Flt3 (A2F10.1), anti-Sca-1 (D7), anti-B220 (RA3-6B2), anti- CD19 (1D3), anti-CD3 (145-2C11), anti-CD4 (GK1.5), anti-CD8 (53–6.7), anti-CDllb (M1/70), anti– Gr-1 (RB6-8C5) and anti-Ter119 (TER119; from BD Biosciences); anti-CD150 (TC15-12F12.2) from Biolegend; anti-CD16/32 (93) from eBioscience; anti-Mpl (AMM2) from IBL. Cells incubated with biotinylated monoclonal antibodies were incubated with fluorochrome-conjugated streptavidin–peridinin chlorophyll protein–cyanine 5.5 (551419; BD) or streptavidin-allophycocyanin-Cy7 (554063; BD). In all the FACS plots, indicated are the percentages (%) of the gated fraction.

4.3. BMT experiments

1×10^6 of bone marrow cells were injected into lethally irradiated (10 Gy) congenic ($CD45.1^+$) recipient mice. For competitive-repopulation experiments, 5×10^5 BM cells from either control or KO mice were mixed with 5×10^5 of WT ($CD45.1^+$) BM cells (to obtain a ratio of 1:1) and were injected into lethally irradiated congenic WT ($CD45.1^+$) recipient mice.

For serial transplantation assays, 1×10^6 of bone marrow cells were injected into lethally irradiated (10 Gy) WT congenic ($CD45.1^+$) recipient mice. After 12 weeks of transplantation, 1×10^6 BM cells of primary recipients were injected into lethally irradiated WT congenic secondary recipients.

4.4. Apoptosis assay

Apoptotic cells were detected by Annexin V PE Apoptosis Detection Kit according to the manufacturer's instructions (BD Bioscience).

4.5. Cell proliferation experiments

For bromodeoxyuridine (BrdU) assay, 3.33 mg of BrdU (BD Pharmingen) was injected intraperitoneally and mice were maintained on 0.8 mg/ml BrdU in the drinking water. After

16 h of injection, mice were sacrificed and bone marrow cells were stained for BrdU, following the BrdU Flow Kit manufacturer's instructions (BD Pharmingen).

4.6. Cell cycle analysis

Cells were stained with surface markers and fixed and permeabilized with Cytofix/Cytoperm fixation/permeabilization solution kit (BD). These cells were stained with Ki-67 (B56;BD) for 30 min and subsequently stained with 20 μg/ml Hoechst 33342 for 5 min and analyzed by flow cytometry.

4.7. ELISA studies

Levels of IFNγ in the blood sera were analyzed using IFNγ ELISA Set (BD Biosciences), according to manufacturer's instructions.

4.8. RNA extraction, PCR, and real-time PCR

Total RNA was isolated with an RNeasy Mini kit or RNeasy Micro kit (QIAGEN). cDNA was synthesized with Oligo(dT) primer and Maxima reverse transcription (Thermo Fisher Scientific). PCR was performed with T100 thermal cycler (Bio-Rad Laboratories) and TSG Taq (Lamda Biotech). Real-time PCR was performed in duplicates with a CFX-connect real-time PCR system (Bio-Rad Laboratories) and SsoAdvanced SYBR Green Supermix (Bio-Rad Laboratories) according to the manufacturer's instructions. Relative expression was normalized to the expression levels of the internal control (housekeeping gene) Hprt.

4.9. Statistics

Data represent mean and s.e.m. Two-tailed student's *t*-tests were used to assess statistical significance (*P < .05, **P < .01, *** < 0.001). For survival curve analysis, log rank test was used to assess statistical significance (*P < .05, **P < .01, *** < 0.001).

Supplementary Material

Refer to Web version on PubMed Central for supplementary material.

Acknowledgements

We thank Drs. Bleul and Boehm for providing the Flt3-Cre mice. This work was supported by grants from the NHLBI HL132194 (CVR).

References

Baldridge MT, King KY, Boles NC, Weksberg DC, Goodell MA, 2010. Quiescent haematopoietic stem cells are activated by IFN-gamma in response to chronic infection. Nature 465, 793–797. [PubMed: 20535209]

Baldridge MT, King KY, Goodell MA, 2011. Inflammatory signals regulate hematopoietic stem cells. Trends Immunol. 32, 57–65. [PubMed: 21233016]

Benz C, Martins VC, Radtke F, Bleul CC, 2008. The stream of precursors that colonizes the thymus proceeds selectively through the early T lineage precursor stage of T cell development. J. Exp. Med. 205, 1187–1199. [PubMed: 18458114]

Boyer SW, Schroeder AV, Smith-Berdan S, Forsberg EC, 2011. All hematopoietic cells develop from hematopoietic stem cells through Flk2/Flt3-positive progenitor cells. Cell Stem Cell 9, 64–73. [PubMed: 21726834]

de Bruin AM, Demirel O, Hooibrink B, Brandts CH, Nolte MA, 2013. Interferon-gamma impairs proliferation of hematopoietic stem cells in mice. Blood 121, 3578–3585. [PubMed: 23487025]

de Bruin AM, Voermans C, Nolte MA, 2014. Impact of interferon-gamma on hematopoiesis. Blood 124, 2479–2486. [PubMed: 25185711]

Cabezas-Wallscheid N, Klimmeck D, Hansson J, Lipka DB, Reyes A, Wang Q, Weichenhan D, Lier A, von Paleske L, Renders S, et al. , 2014. Identification of regulatory networks in HSCs and their immediate progeny via integrated proteome, transcriptome, and DNA methylome analysis. Cell Stem Cell 15, 507–522. [PubMed: 25158935]

Cheung TH, Rando TA, 2013. Molecular regulation of stem cell quiescence. Nat. Rev. Mol. Cell Biol. 14, 329–340. [PubMed: 23698583]

Essers MA, Offner S, Blanco-Bose WE, Waibler Z, Kalinke U, Duchosal MA, Trumpp A, 2009. IFNalpha activates dormant haematopoietic stem cells in vivo. Nature 458, 904–908. [PubMed: 19212321]

Hitotsumatsu O, Ahmad RC, Tavares R, Wang M, Philpott D, Turer EE, Lee BL, Shiffin N, Advincula R, Malynn BA, et al. , 2008. The ubiquitin-editing enzyme A20 restricts nucleotide-binding oligomerization domain containing 2-triggered signals. Immunity 28, 381–390. [PubMed: 18342009]

Hymowitz SG, Wertz IE, 2010. A20: from ubiquitin editing to tumour suppression. Nat. Rev. Cancer 10, 332–341. [PubMed: 20383180]

Kim KH, Sederstrom JM, 2015. Assaying cell cycle status using flow cytometry. Curr. Protoc. Mol. Biol. 111 (28) 26 21–11. [PubMed: 26131850]

King KY, Goodell MA, 2011. Inflammatory modulation of HSCs: viewing the HSC as a foundation for the immune response. Nat. Rev. Immunol. 11, 685–692. [PubMed: 21904387]

Matsumoto A, Takeishi S, Kanie T, Susaki E, Onoyama I, Tateishi Y, Nakayama K, Nakayama KI, 2011. p57 is required for quiescence and maintenance of adult hematopoietic stem cells. Cell Stem Cell 9, 262–271. [PubMed: 21885021]

Mirantes C, Passegue E, Pietras EM, 2014. Pro-inflammatory cytokines: emerging players regulating HSC function in normal and diseased hematopoiesis. Exp. Cell Res. 329, 248–254. [PubMed: 25149680]

Nakagawa MM, Thummar K, Mandelbaum J, Pasqualucci L, Rathinam CV, 2015. Lack of the ubiquitin-editing enzyme A20 results in loss of hematopoietic stem cell quiescence. J. Exp. Med. 212, 203–216. [PubMed: 25624445]

Sato T, Onai N, Yoshihara H, Arai F, Suda T, Ohteki T, 2009. Interferon regulatory factor-2 protects quiescent hematopoietic stem cells from type I interferon-dependent exhaustion. Nat. Med. 15, 696–700. [PubMed: 19483695]

Shen H, Boyer M, Cheng T, 2008. Flow cytometry-based cell cycle measurement of mouse hematopoietic stem and progenitor cells. Methods Mol. Biol. 430, 77–86. [PubMed: 18370292]

Snapper CM, Yamaguchi H, Urban JF Jr., and Finkelman FD (1991). Induction of Ly-6A/E expression by murine lymphocytes after in vivo immunization is strictly dependent upon the action of IFN-alpha/beta and/or IFN-gamma. Int. Immunol. 3, 845–852. [PubMed: 1931812]

Sun SC, 2008. Deubiquitylation and regulation of the immune response. Nat. Rev. Immunol. 8, 501–511. [PubMed: 18535581]

Vereecke L, Beyaert R, van Loo G, 2009. The ubiquitin-editing enzyme A20 (TNFAIP3) is a central regulator of immunopathology. Trends Immunol. 30, 383–391. [PubMed: 19643665]

Weiner RS, Pelayo R, Nagai Y, Garrett KP, Wuest TR, Carr DJ, Borghesi LA, Farrar MA, Kincade PW, 2008. Lymphoid precursors are directed to produce dendritic cells as a result of TLR9 ligation during herpes infection. Blood 112, 3753–3761. [PubMed: 18552210]

Wertz IE, O'Rourke KM, Zhou H, Eby M, Aravind L, Seshagiri S, Wu P, Wiesmann C, Baker R, Boone DL, et al. , 2004. De-ubiquitination and ubiquitin ligase domains of A20 downregulate NF-kappaB signalling. Nature 430, 694–699. [PubMed: 15258597]

Wilson A, Laurenti E, Oser G, van der Wath RC, Blanco-Bose W, Jaworski M, Offner S, Dunant CF, Eshkind L, Bockamp E, et al. , 2008. Hematopoietic stem cells reversibly switch from dormancy to self-renewal during homeostasis and repair. Cell 135, 1118–1129. [PubMed: 19062086]

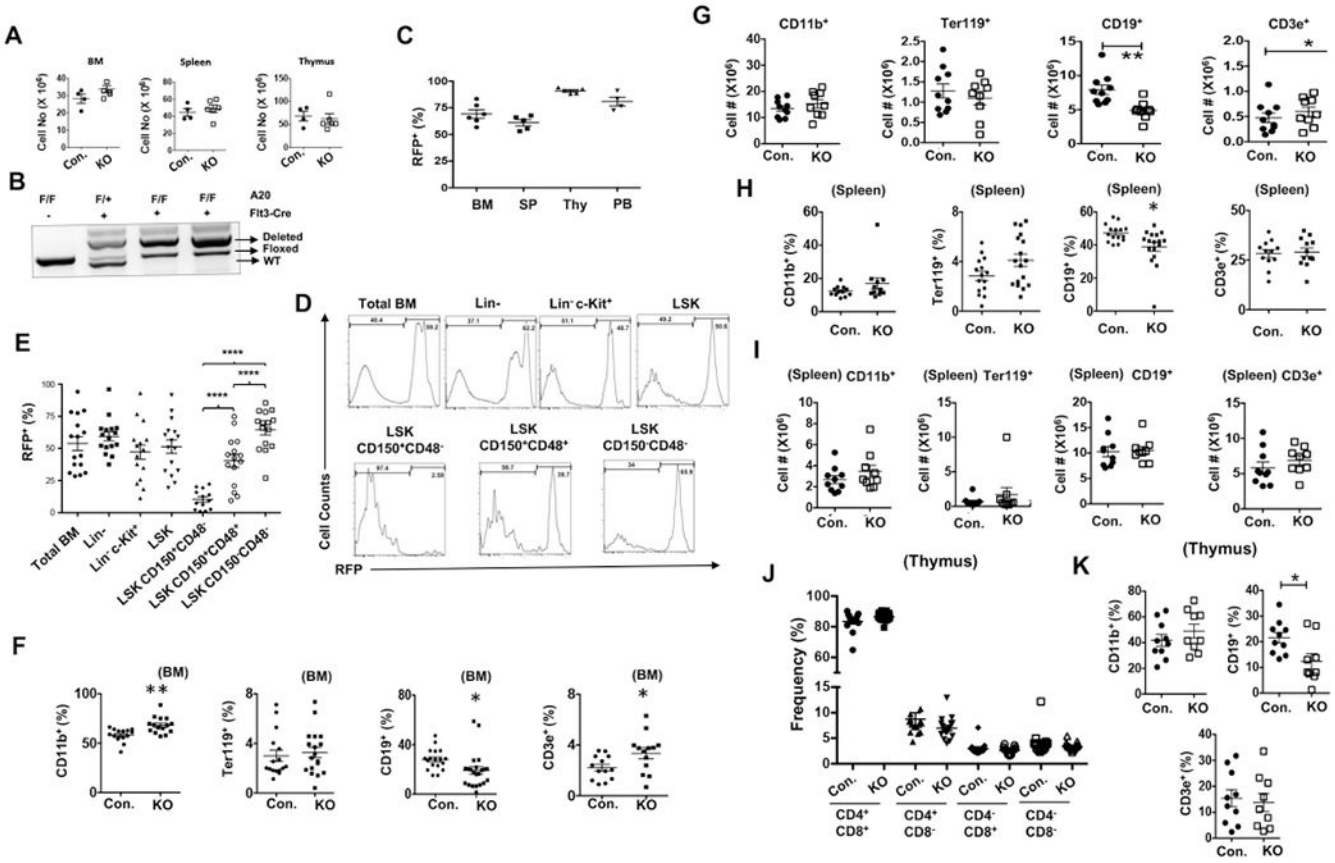

Fig. 1.

A20 deficiency in MPPs leads to modest changes in hematopoiesis. (A) Cellularity of BM (two femurs and two tibias), thymus and spleen of 8 weeks old $A20^{F/F}Flt3^{cre/+}$ and control mice (n = 4–6). (B) Genotyping PCR for Tnfaip3 gene from BM of A20F/FFlt3+/+, A20F/+Flt3cre/+ and A20F/FFlt3cre/+ mice. (C) Frequencies of RFP+ cells in the indicated hematopoietic organs from A20F/FFlt3cre/+ RosaRFP mice. (D) Representative histograms indicating frequencies of RFP+ cells in the specified hematopoietic subsets from A20F/FFlt3cre/+ RosaRFP mice. (E) Cumulative data indicating frequencies of RFP+ cells in hematopoietic subsets of A20F/FFlt3cre/+ RosaRFP mice (n = 15–16). (F) Frequencies of CD11b+, Ter119+, CD19+ and CD3e+, cells in the BM of A20F/FFlt3cre/+ and control mice (n = 13–18).

(G) Absolute number of myeloid cells (CD11b+, 1st panel), erythroid cells (Ter119+, 2nd panel), B cells (CD19+, 3rd panel) and T cells (CD3+, 4th panel) from the BM of 8 weeks old A20F/FFlt3cre/+ and control mice (n = 9–10). (H) Frequencies of CD11b+, Ter119+, CD19+ and CD3e+, cells in the Spleen of A20F/FFlt3cre/+ and control mice (n = 12–17). (I) Absolute number of myeloid cells (CD11b+, 1st panel), erythroid cells (Ter119+, 2nd panel), B cells (CD19+, 3rd panel) and T cells (CD3+, 4th panel) from the spleen of 8 weeks old A20F/FFlt3cre/+ and control mice (n = 9–10). (J) Frequencies of CD4+CD8+, CD4+CD8−, CD4−CD8+ and CD4−CD8− in the thymus of A20F/FFlt3cre/+ and control mice (n = 11–15). (K) Frequencies of myeloid cells (CD11b+, 1st panel), B cells (CD19+, 2nd panel) and T cells (CD3+, 3rd panel) from the peripheral blood of 8 weeks old

A20F/FFlt3cre/+ and control mice (n = 9–10). All data represent mean ± SEM. Two-tailed student's *t*-tests were used to assess statistical significance (*P < .05, **P < .01, *** P < .001).

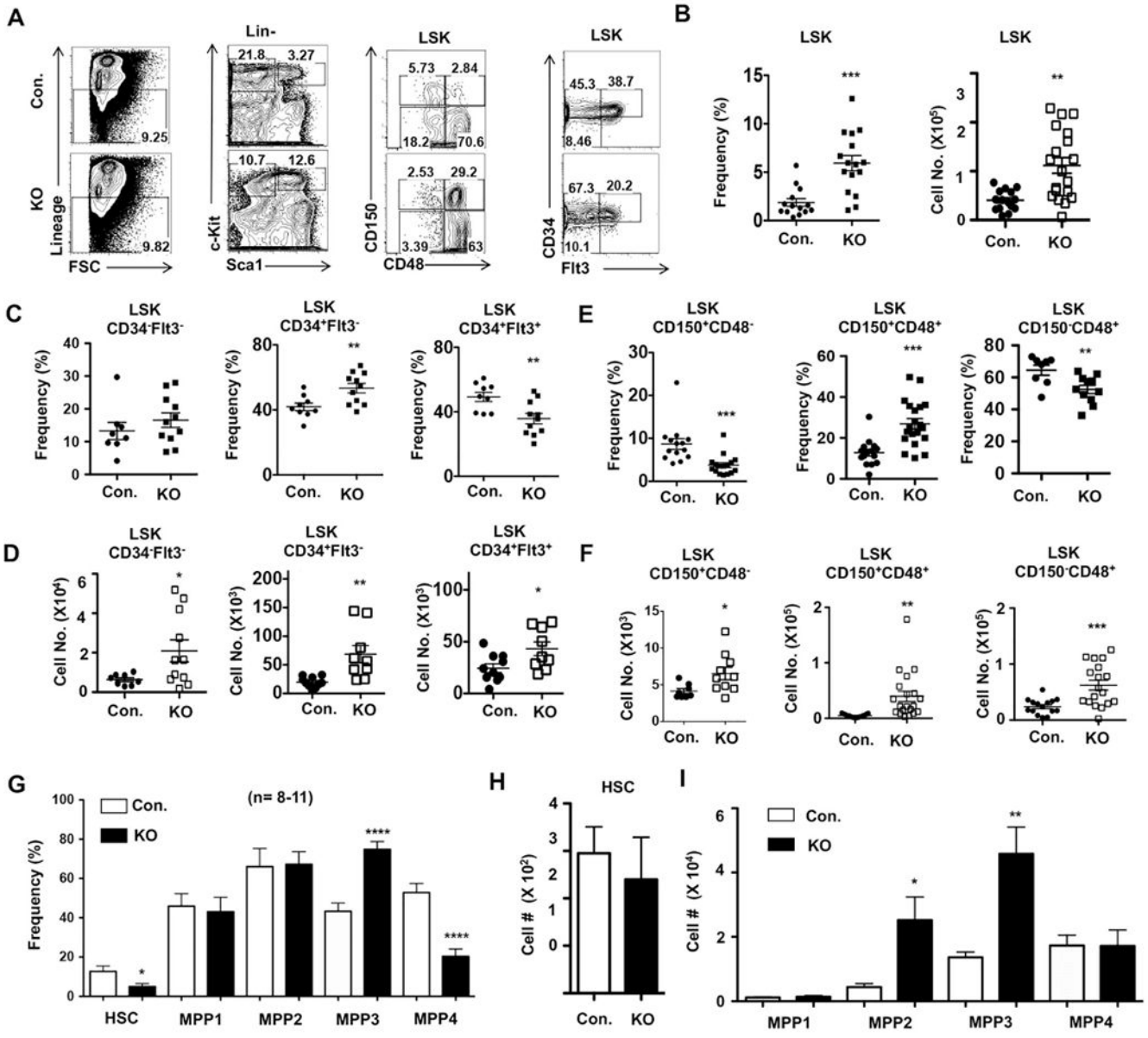

Fig. 2.

Lack of A20 in MPPs affects maintenance of HSPC pool. (A) Representative FACS plots for hematopoietic stem cells and progenitors of the BM from 8 weeks old A20F/FFlt3cre/+ and control mice. (B) Relative frequencies and absolute numbers of LSK cells in the BM of 4–8 weeks old A20F/FFlt3cre/+ (n = 16) and control (n = 14) mice. (C & D) Relative frequencies (C) and absolute numbers (D) of CD34−Flt3−LSK, CD34+Flt3−LSK and CD34+Flt3+LSK subsets in the BM of 4–8 weeks old A20F/FFlt3cre/+ (n = 11) and control (n = 8) mice. (E & F) Relative frequencies (E) and absolute numbers (F) of CD150+CD48−LSK, CD150+CD48+LSK and CD150−CD48+LSK subsets in the BM of 4–8 weeks old A20F/FFlt3cre/+ (n = 16) and control (n = 9) mice. (G–I) Relative frequencies (G) and absolute numbers (H&I) of HSCs (CD150+CD48-CD34-Flt3-LSK) (H), MPP1 (CD150+CD48-CD34+Flt3-LSK), MPP2 (CD150+CD48+CD34+Flt3-LSK), MPP3

(CD150-CD48+CD34+Flt3-LSK) and MPP4 (CD150-CD48+CD34+Flt3+LSK) (I) subsets in the BM of 4–8 weeks old A20F/FFlt3cre/+ (n = 11) and control (n = 8) mice. All data represent mean ± SEM. Two-tailed student's *t*-tests were used to assess statistical significance (*P < .05, **P < .01, *** P < .001).

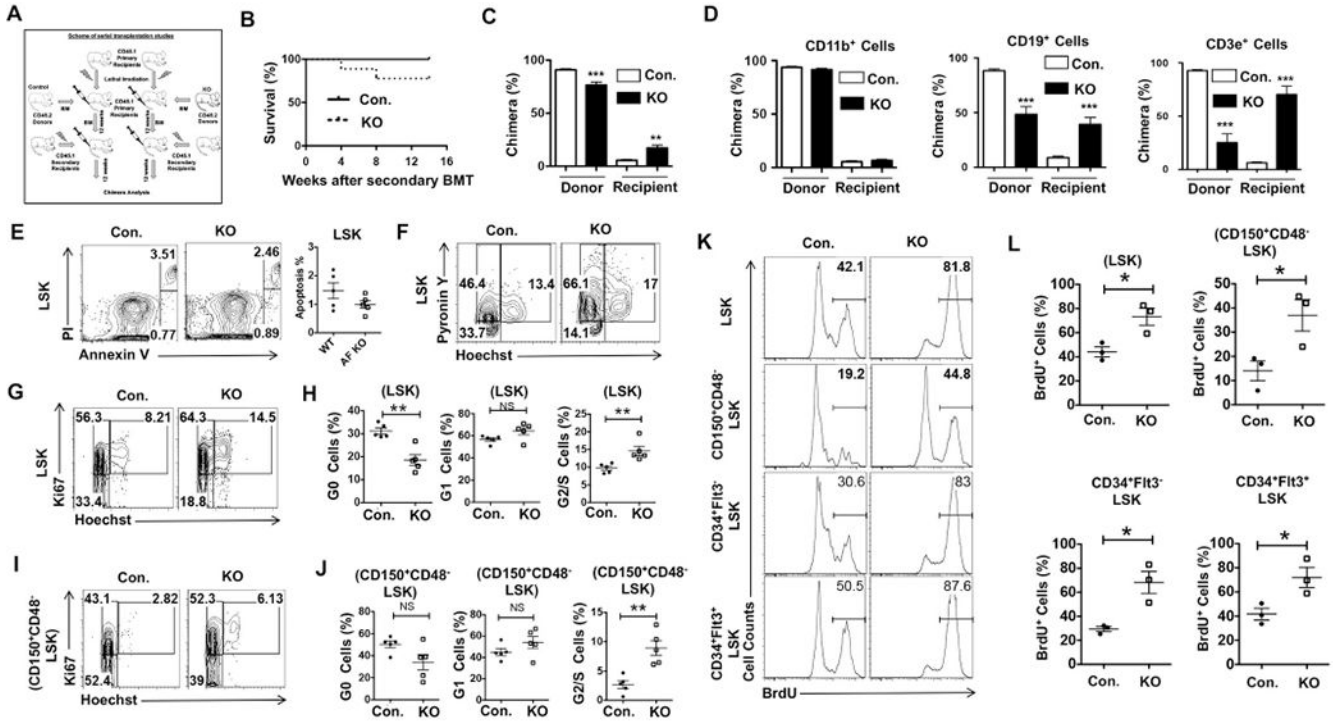

Fig. 3.

Loss of A20 in MPPs leads to loss of quiescence of HSPCs. (A) Schematic of serial transplantation experiments. (B) Survival curve of lethally-irradiated WT congenic (CD45.1+) secondary recipients (n = 9). Total BM cells from A20F/FFlt3cre/+ and control groups were injected into lethally irradiated WT congenic primary recipients (n = 10). After 12 weeks of transplantation primary recipients were sacrificed and their BM cells were injected into lethally irradiated WT congenic secondary recipients (n = 9). (C) Frequencies of donor (CD45.2+)-derived cells in the peripheral blood of secondary recipients after 12 weeks of BMT (n = 7). (D) Frequencies of donor (CD45.2+) and recipient (CD45.1+) derived CD11b+ , CD19+ and CD3e+ cells in the peripheral blood of secondary recipients at 12 weeks of transplantation (n = 7). (E) Apoptosis assay of LSK cells from the BM of 8 weeks old A20F/FFlt3cre/+ and control mice (n = 5). Representative FACS plots (left) and dot plots (right). (F) Cell cycle analysis (Hoechst and Pyronin Y) of LSK cells from the BM of 8 weeks old A20F/FFlt3cre/+ and control mice. (G–J) Cell cycle analysis (Hoechst and Ki67) of LSK cells (G and H) and CD150+ CD48− LSK cells (I and J) from the BM of 8 weeks old A20F/FFlt3cre/+ and control mice. Representative FACS plots (G and I) and dot plots (H and J) (n = 5). (K and L) BrdU assay of HSPCs from the BM of 8 weeks old A20F/FFlt3cre/+ and control mice (n = 3). Representative FACS plots (K) and dot plots (L). All data represent mean ± SEM. Two-tailed student's *t*-tests were used to assess statistical significance (*P < .05, **P < .01, *** P < .001).

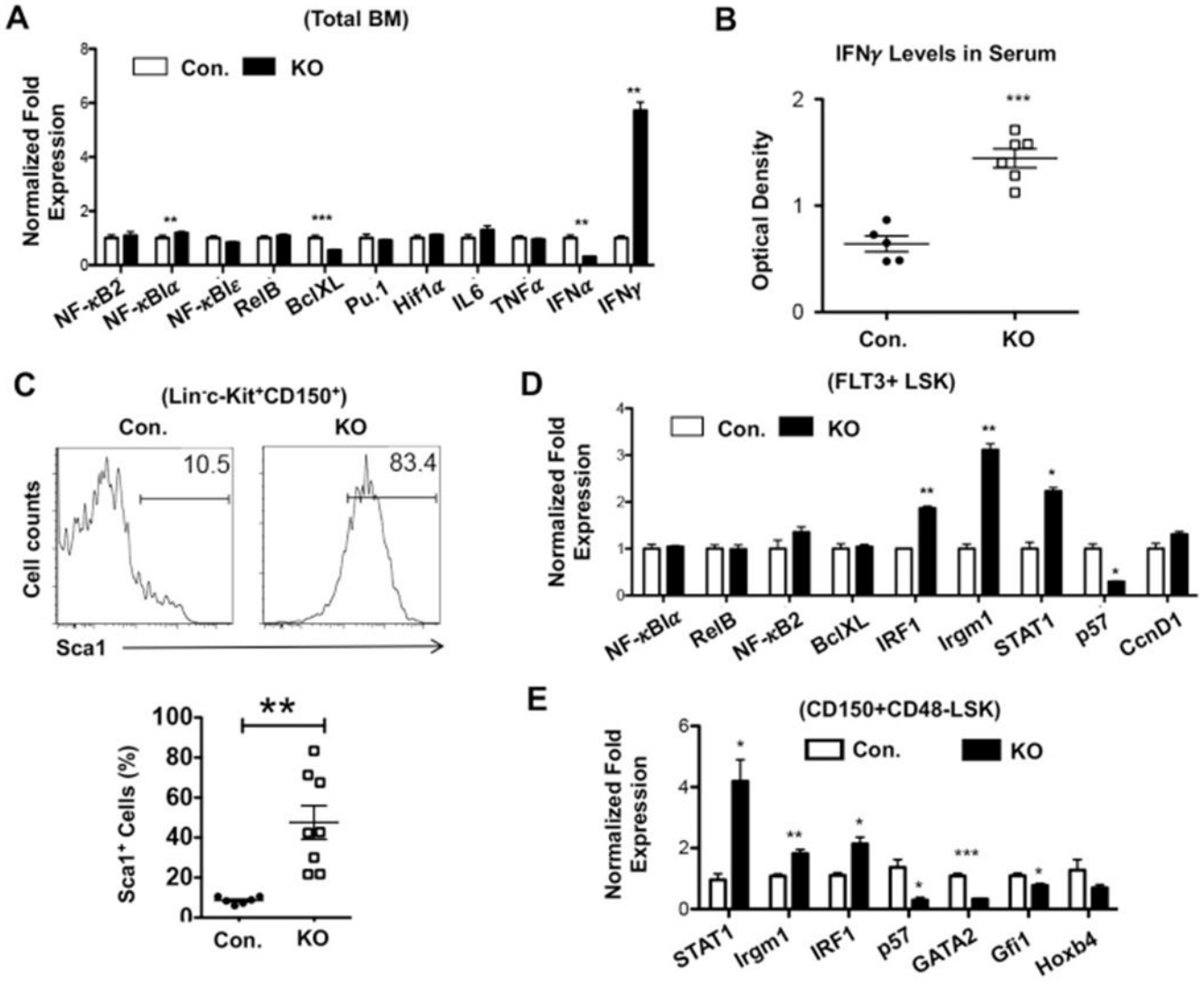

Fig. 4.

A20 deficiency leads to exaggerated IFNγ expression and signaling in HSPCs. (A) Relative expression of indicated targets in the total BM cells of 8 weeks old A20F/FFlt3cre/+ and control mice. Expression levels of target genes were normalized to HPRT levels. Data are representative of 3 independent experiments. (B) ELISA data documenting IFNγ levels in the serum of 8 weeks old A20F/FFlt3cre/+ and control mice (n = 5–6) (C) Representative FACS plots (top) and cumulative frequencies (bottom) indicating expression levels of Sca-1 in Lin-c-Kit+CD150+ cells of the BM from 8 weeks old A20F/FFlt3cre/+ and control mice (n = 6–8). (D & E) Relative expression of indicated targets in Flt3+LSK cells (D) and CD150+CD48-LSK cells (E) of 8 weeks old A20F/FFlt3cre/+ and control mice. Expression levels of target genes were normalized to HPRT levels. Data are representative of 2 (D) and 3 (E) independent biological replicates. All data represent mean ± SEM. Two-tailed student's *t*-tests were used to assess statistical significance (*P < .05, **P < .01, *** P < .001).